

Climate Dynamics in Deep Time: Modeling the “Snowball Bifurcation” and Assessing the Plausibility of its Occurrence

W. R. Peltier, L. Tarasov, and G. Vettoretti

Department of Physics, University of Toronto, Toronto, Ontario, Canada

L. P. Solheim

Canadian Climate Centre for Modeling and Analysis, University of Victoria, Victoria, British Columbia, Canada

The apparently global scale glaciation events that occurred during the Neoproterozoic era, in the interval from 750 Ma to 550 Ma, represent a significant challenge to our understanding of climate system behavior. If these episodes of glaciation were truly of “snowball” type, with the continents covered by thick ice-sheets and the oceans entirely capped by sea ice, then special pleading is required to understand the Cambrian explosion of life that occurred subsequently. Detailed models of Neoproterozoic climate, however, suggest the plausibility of preference for “equatorial refugium” or “oasis” solutions in which significant regions of open water are able to persist at the equator. We describe further analyses of such solutions in this paper, using both simple EBM coupled ice sheet models and fully articulated atmosphere-ocean-sea ice coupled models of climate evolution. Recently published analyses of the dynamics of the Neoproterozoic carbon cycle, taken together with the predictions of the models discussed herein, are strongly supportive of the equatorial refugium solutions as the most plausible form of the Neoproterozoic cooling events.

1. INTRODUCTION

The notion that the Earth was once entombed in a state of global glaciation is one that has episodically re-emerged in the geological and geophysical literature since the idea was first advocated by *Louis Agassiz* [1842]. As with the more recent proponents of the idea [e.g. *Kirschvink*, 1992; *Hoffman and Schrag*, 2002], Agassiz argued the necessity of this interpretation (die Eiszeit) on the basis of a belief [Agassiz, 1866] that continental glaciation had occurred at low tropical lati-

tudes. His focus was upon the Amazon region of Brazil. As we have been reminded in the recent review of the now burgeoning “snowball literature” by *Eyles and Januszczak* [2003], Agassiz’s argument was eventually shown to be invalid by *Branner* [1893]. His error of interpretation was traced to a false conclusion that a boulder laden clay found in this geographical region was glacially produced, whereas it was in fact a simple consequence of igneous rocks having been subjected to deep weathering.

The most recent resurrection of the “snowball Earth” idea, as represented in the review by *Hoffman and Schrag* [2002], also has precedents in the work of *Harland and Herod* [1975] and *Chumakov* [1981]. It has deservedly received more serious attention than these previous formulations, however, because it has been accompanied by the elaboration of a seemingly

plausible scenario involving climate system interactions that are not simple to dismiss on a-priori grounds. The most fundamental underpinnings of this scenario are to be found in geological data related to the carbon cycle, specifically in the time dependence of the ratio of ^{13}C to ^{12}C , denoted $\delta^{13}\text{C}$, and measured over long geological timescales in carbonates assumed to have been precipitated from the oceans and assumed to be measuring the isotopic fractionation association with photosynthesis. The measurement is therefore, in some sense, a measure of biological activity. Plate 1, based upon *Kauffman* [1997] and *Hoffman and Schrag* [1999], places these data in both a tectonophysical and a glaciological context. The Plate illustrates the temporal relationships between the very large amplitude oscillations in $\delta^{13}\text{C}$ that occurred between 750 Ma and 550 Ma in the Neoproterozoic, and the geological evidence for the times of occurrence of significant continental glaciation and the times during which supercontinents were being constructed and later “rifted” asunder. It will be noted that the Neoproterozoic era which is characterized by the large amplitude oscillations of $\delta^{13}\text{C}$ is entirely unique during the most recent 1.6 Ga of Earth history. Notable also is the fact that this era immediately preceded the beginning of the Cambrian period and the so called “Cambrian explosion of life” that occurred during it. One reason for the significant current level of interest in the snowball Earth hypothesis concerns the connection that might exist between a global freezing event and the onset of rapid evolutionary diversification that took place in its aftermath. The implausibility of this having occurred, from a biological perspective, has been stressed by *Runnegar* [2000] who referred to the snowball Earth hypothesis as “a script for global catastrophe”.

Now the data shown on Plate 1 would appear to establish that there was indeed something rather special about the carbon cycle during the Neoproterozoic and it is equally clear that this interval in Earth history was one during which continental glaciation was extreme, if episodic. It is therefore unsurprising that the climate system interactions invoked by *Hoffman and Schrag* [2000] to support the plausibility of the occurrence of a “hard snowball” event or events have been focused upon atmospheric carbon dioxide, as well as upon the more obvious candidate for cooling based upon the secular variation in solar radiation. The latter contribution may be understood to be known on the basis of standard models of the evolution of main sequence stars such as our own Sun, models that predict the outgoing flux of energy, integrated over wavenumber, to increase at a rate of approximately 1% per 100 My as the star ages. The former contribution, however, is very much more poorly known, the best available model apparently being the GEOCARB model due to *Berner* [e.g. 1994]. This model, for which the time variation of CO_2 over the Phanerozoic period is shown on Figure 1, has been found to be difficult to

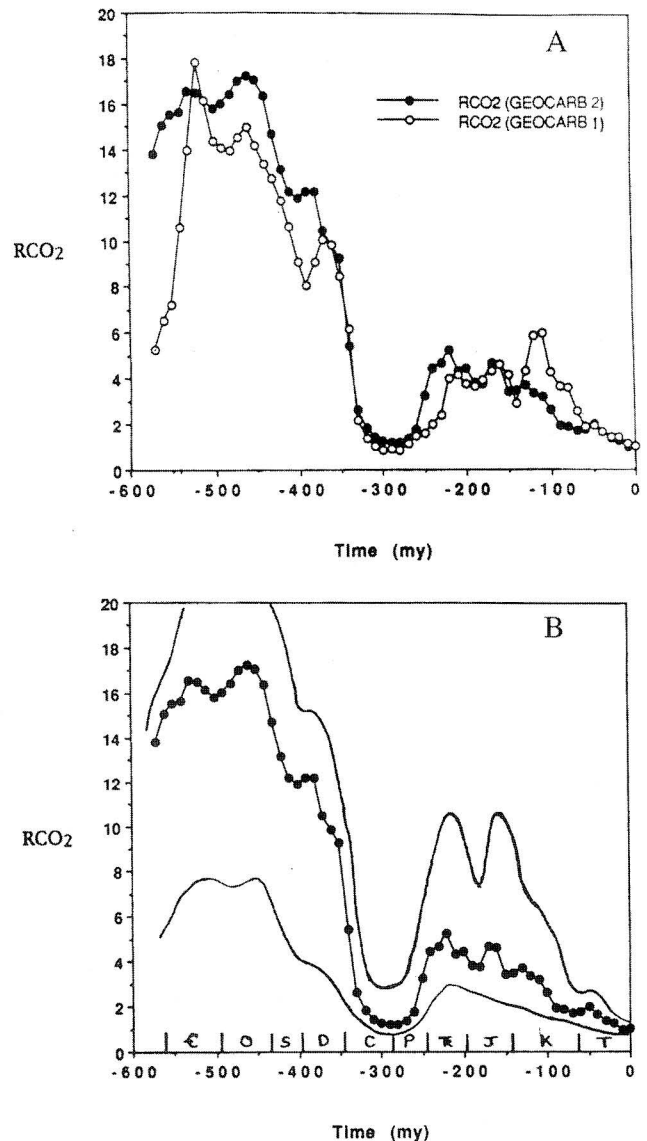


Figure 1. (A) The variation of the atmospheric concentration of carbon dioxide over the Phanerozoic era according to the GEOCARB I and GEOCARB II models of *Berner* [e.g. 1994]. Reproduced from *Berner* [1994] with permission. (B) Approximate error bounds upon the atmospheric CO_2 concentration according to the GEOCARB II reconstruction.

extend into the Neoproterozoic and so the issue of the concentration of CO_2 in the atmosphere that accompanied the $\delta^{13}\text{C}$ oscillations shown on Plate 1 remains open and has proven to provide fertile ground for speculation. During Phanerozoic time, however, it is clearly interesting and relevant to note that the minimum of atmospheric pCO_2 that occurred during the Carboniferous period at approximately 300 Ma, according to *Berner*, was coincident with the glacia-

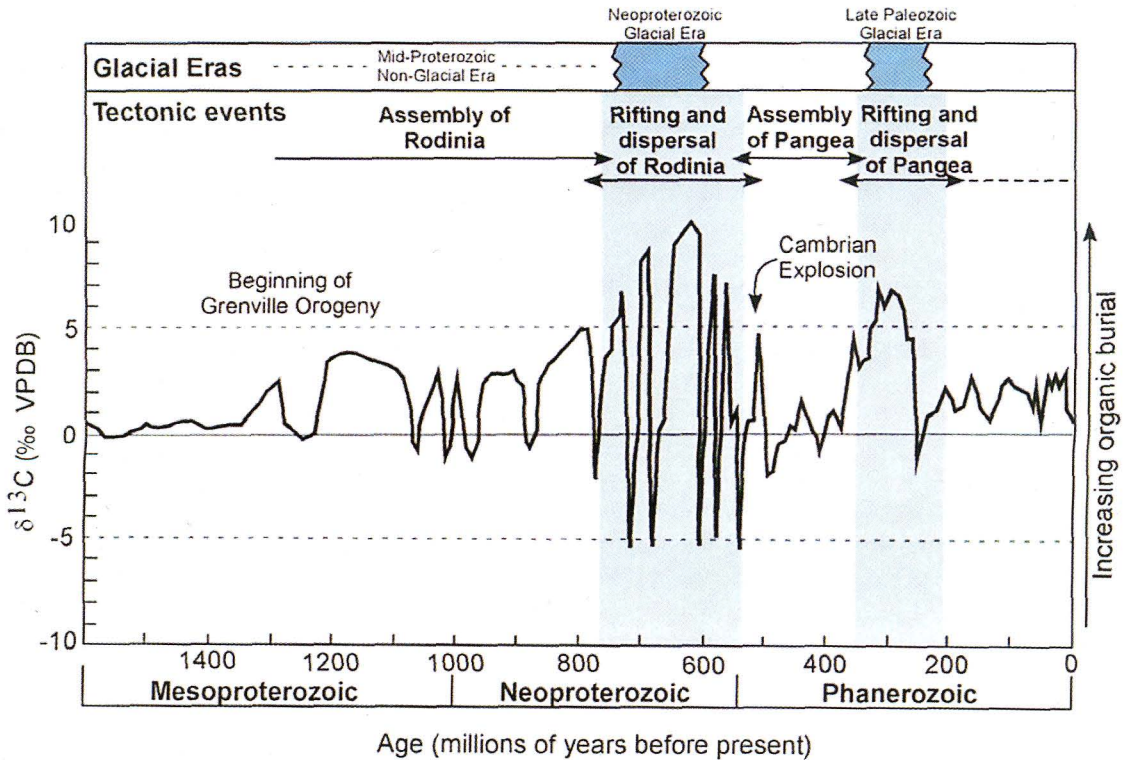


Plate 1. The variation of carbon isotopes, denoted $\delta^{13}\text{C}$, over the last 1.6 Ga of Earth history shown together with the times of occurrence of periods of significant continental glaciation and the times of creation and destruction of super continents that accompany the so-called “Wilson Cycle”. The $\delta^{13}\text{C}$ time series is from *Kauffman* [1997] and *Hoffman and Schrag* [1999] as modified in *Eyles and Januszczak* [2003] (reproduced with permission).

tion of the supercontinent of Pangea and that the current minimum of the past few Ma has been coincident with the quasi-permanent glaciations of Greenland and Antarctica and, in the past million years, with a continuous, orbitally driven, 100 kyr oscillation of glaciation of the northern hemisphere continents near the rotation pole. To the extent that the GEOCARB model is a reasonable approximation of reality, we might therefore be forgiven for concluding that episodes of significant continental glaciation through Earth history occurred under conditions of reduced atmospheric $p\text{CO}_2$. It is important to recognize, however, that the GEOCARB model is not the only model of the variation of Phanerozoic atmospheric carbon dioxide concentration. In particular there are those of *Bodyko et al.* [1987] and *Rothman* [2002], models which do differ significantly from that of Berner.

Although the GEOCARB model does not extend into the Neoproterozoic, there is nevertheless good reason to believe that times of sharply varying $\delta^{13}\text{C}$ may correspond to times of sharply varying atmospheric $p\text{CO}_2$. Again, this is a consequence of the fact that when the photosynthetic process that is primarily responsible for the isotopic fractionation represented by $\delta^{13}\text{C}$ is active, carbon is being stored in the organic form and burial rates are high. The process of remineralization of the organic reservoir in the presence of oxygen produces CO_2 whereas the process of photosynthesis consumes it. There is therefore the possibility of occurrence of a CO_2 oscillation which has recently been suggested on the basis of entirely different lines of argument by *Crowley et al.* [2001] and *Rothman et al.* [2003], an oscillation that would have to rely upon the nonlinearity of the coupled physical-biogeochemical climate system for its existence. In this paper our goal will be to seek an understanding in terms of climate dynamics for the occurrence of these $\delta^{13}\text{C}$ oscillations that were such a prominent feature of the Neoproterozoic period of Earth history. The development of a climate dynamical interpretation of the ideas of *Crowley et al.* [2001] and *Rothman et al.* [2003] will form a prominent focus of the work to be discussed in the present paper.

As clearly illustrated by the data shown on Plate 1, however, the apparently oscillatory variations in the carbon cycle are not the only distinguishing feature of the Neoproterozoic period. It is clearly also important that the continents upon which glaciation was occurring during this period were being massively re-organized as the supercontinent of Rodinia underwent the two episodes of rifting that split it into a multiplicity of fragments that were then dispersed by the action of the mantle convection process. In fact, as recently discussed in some detail by *Eyles and Januszczak* [2003], the two most prominent glaciations that are supposed to have occurred in Neoproterozoic time, respectively the Sturtian ice age which occurred in the interval $\sim 760\text{--}700$ Ma and the Veranger (or

Marinoan) ice age that occurred in the interval $\sim 620\text{--}580$ Ma, occurred during intervals coincident with the two stages of rifting that led to the complete breakup of Rodinia. Their work has emphasized the role that tectonics may well have played in the individual glaciation events, and in generating the sedimentological characteristics of the geological sections that are supposed by *Hoffman and Schrag* [e.g. 2000] to provide the irrefutable evidence that snowball glaciation actually occurred. An important component of the climate dynamic scenario of *Hoffman and Schrag* [2000] is the explanation of the so-called “cap carbonates” that are found, on occasion, to overlie the supposed glacial deposits of Neoproterozoic age. Their suggestion is that these rocks were formed once the influence of continuous volcanic outgassing into the atmosphere under “hard snowball” conditions had become such as to raise the atmospheric CO_2 sufficiently that the enhanced greenhouse effect was able to rapidly eliminate the global cover of sea ice. *Eyles and Januszczak* [2003] provide compelling counter argument to the effect that the diamictites that have been interpreted as glacial by the proponents of the snowball hypothesis are more likely to have been produced by debris flows driven downslope off the uplifted margins produced by rifting of the supercontinent. In arguing in this way the authors are suggesting that, just as Agassiz was misled in his interpretation of the boulder laden clay in Amazonia, Hoffman and others may also have been misled in their interpretation of the sedimentological evidence of low latitude and therefore necessarily “snowball” glaciation. These authors have also provided an alternative interpretation of the cap carbonates themselves.

One way in which we might hope to better understand the climate regime that existed during the Neoproterozoic is to employ climate system models to compute the state of the coupled atmosphere-ocean-cryosphere system that should have obtained under Neoproterozoic conditions. Although this approach to the problem of assessing the plausibility of occurrence of the snowball bifurcation is fraught with its own difficulties, such an approach is nevertheless one based upon first principles and is therefore useful counterpoint to the similarly complex process of geological inference. Issues that must be addressed involve our incomplete knowledge of the continental configuration that existed during either of the primary Neoproterozoic glacial events, our total lack of knowledge of the atmospheric concentrations of the greenhouse gases during this interval of time, as well as our total lack of knowledge of the bathymetry of the ocean basins.

The approach that we will take in the analyses to be discussed in what follows will be to employ two different models of the climate system to investigate the plausibility of occurrence of hard snowball events of the kind that have been hypothesized by Hoffman and colleagues. One of these will

be the same energy balance model (EBM) coupled to a model of continental scale glaciology that has been developed at Toronto to successfully explain the 100 kyr ice age cycle of the late Pleistocene [e.g. *Deblonde and Peltier, 1993, Tarasov and Peltier, 1999*] as well as the Carboniferous glaciation of Pangea [*Hyde et al. 1999*]. The second model to be employed will be the complete coupled atmosphere-ocean-sea ice-land surface processes model that has been developed at the National Center for Atmospheric Research (NCAR) in Boulder, Colorado and which will be referred to herein as the Community Climate System Model (CCSM). By intercomparing the results obtained by the application of these two different representations of climate system behavior, we may hope to better understand the robustness of the predictions that models make concerning Neoproterozoic climate. As will become evident, this issue turns out to be important.

In the following Section of this paper we will briefly summarize the properties of the two models that will be employed for the purpose of subsequent analysis, as well as the design of the numerical experiments to be performed with them. Section 3 of the paper describes the new results that have been obtained using each model, whereas Section 4 provides a discussion of the climate dynamical interpretation of the $\delta^{13}\text{C}$ oscillations that follows from these model based analyses. Our conclusions are presented in Section 5.

2. MODELS OF NEOPROTEROZOIC CLIMATE AND DESIGN OF THE NUMERICAL EXPERIMENTS

Since fairly complete descriptions of both of the models to be employed for the purpose of the present work have already appeared in the literature, the level of detail concerning them to be provided here will be minimal. Interested readers should consult the citations given if they wish to read more complete discussions of technical details.

2.1. The Ice Sheet Coupled Energy Balance Model (EBM/ISM)

As previously mentioned, this model has its origins in work at Toronto directed towards the development of a theory of the 100 kyr cycle of late Pleistocene continental ice volume. The current version of this model, most recently employed to predict the evolutionary history of the North American and Eurasian ice sheets over the last glacial cycle [*Tarasov and Peltier, 1999, Peltier, 2002*], differs from the version of the model employed in *Hyde et al. [2000]* to investigate Neoproterozoic climate in that the ice sheet component of the model is a full three dimensional thermomechanical model rather than the simple isothermal model developed in *Deblonde and Peltier [1991, 1993]* and *Deblonde, Hyde and Peltier [1992]*.

The full model consists of several individual elements for which a linked set of nonlinear partial differential equations must be solved. The global EBM is essentially that of *North et al. [1983]* to which has been added a simple thermodynamic sea ice module. This EBM is described by the following nonlinear diffusion equation:

$$C(\underline{r},t) \frac{\partial T_s(\underline{r},t)}{\partial t} = \nabla_h \cdot (D(\theta) \nabla_h T_s) - (A + B T_s) + a(\underline{r},t) \frac{Q}{4} S(\theta,t) \quad (1)$$

In this equation, $C(\underline{r},t)$ is the space and time dependent heat capacity of the surface of the sphere which is employed to distinguish continental from oceanic surface and ice covered from non-ice-covered surface. $T_s(\underline{r},t)$ is the space and time dependent surface temperature, $D(\theta)$ is a latitude dependent diffusion coefficient that is inferred by tuning the model so as to enable it to fit observations of the pole-to-equator variation of temperature under modern climate conditions, the numbers A and B are obtained by linearizing the black body emission relation and tuning A and B so as to fit satellite observations of emitted radiation. The coefficient A may then be modified to represent the reduction or enhancement of the infrared forcing at the surface that arises from a change in the atmospheric carbon dioxide concentration. The space and time dependent function $S(\theta,t)$ represents the variation of the insolation incident at the top of the atmosphere (TOA) which includes the variation due to changes in the parameters that determine the geometry of Earth's orbit around the Sun. The space and time dependent parameter $a(\underline{r},t)$ is the surface albedo which is employed to distinguish a highly reflective surface such as that associated with continental ice or sea ice cover, from less reflective surfaces, either continent or non-sea-ice-covered ocean. $Q \equiv 1370 \text{ W/m}^2$ is the solar constant.

This model of the global energy balance is coupled to a three-dimensional thermo-mechanical model of continental ice-sheet evolution. As is the case with (1), this component of the coupled structure is also described by a non-linear diffusion equation for ice thickness H , as:

$$\frac{\partial H}{\partial t} = - \nabla_h \cdot \int_{z_b}^h \underline{V}(\underline{r}) dz + G(\underline{r}, T(\underline{r})) \quad (2a)$$

where

$$\underline{V}(\underline{r}) = \underline{V}_b(\underline{r}) - 2(\rho_i g)^m \{ \nabla_h(h) \cdot \nabla_h(h) \}^{(m-1)/2} \cdot \nabla_h(h) \cdot \int_{z_b}^z A(T(z')) (h - z')^m dz' \quad (2b)$$

in which h is the surface elevation above present-day sea level, ρ_i is the density of ice, g is the acceleration due to gravity, T is the temperature of the ice, and G is the net mass balance. Both (1) and (2) are solved on the surface of the sphere. In (2), the function $A(T)$ is such that

$$A(T) = f \beta \exp(-Q/R_{gas} T^\#) \quad (3)$$

where f is a flow enhancement factor introduced in order to capture the increases in strain rate due to crystalline anisotropy and/or impurities and where $T^\#$ is the temperature of the ice in degrees Kelvin corrected for the pressure melting point, i.e. $T^\# = T_{ice}(z) - 8.7 \times 10^{-4} (\text{°K/m})(h-z)$. The flow parameter β and activation energy Q are set equal to those defined by the European EISMINT intercomparison project protocols [Payne *et al.* 2000]. The critically important mass balance function $G(\underline{r}, t)$, which consists of both accumulation and ablation components, is computed using a modification of the methodology employed in the 100 kyr cycle analyses discussed in Tarasov and Peltier [1999]. Ablation is computed using the two level PDD (positive degree day) method of Huybrechts and Tsiobbel [1995] whereas precipitation, in the absence of any significant knowledge of this field for the Neoproterozoic period, will be taken to be a globally constant parameter of the model to be varied, as will be the mean elevation of the continents on which continental ice sheets may grow. For the purpose of the Neoproterozoic calculations we have assumed, explicitly, that the local precipitation rate $prec(t)$ was computable as:

$$prec(t) = preco. (1.03)^{T_{sea\ level}(t)}$$

with the standard value for $preco$ taken to be 0.6 m/yr.

The final component of the ice-sheet coupled EBM consists of a model of the glacial isostatic adjustment (GIA) process, a physical process that influences ice sheet topography in an important way through the so-called elevation desert effect. As the surface of the solid Earth sinks under the weight of an applied ice load, the surface of the ice-sheet itself moves to a lower elevation with respect to sea level than it would otherwise occupy, thus entering a regime of higher precipitation than would otherwise be the case. In the version of the ice-sheet coupled EBM to be employed herein, the GIA process will be described using a simple “damped return to equilibrium” model that has the following mathematical form:

$$\frac{\partial h'}{\partial t} = \frac{(h'(\underline{r}, t) - h_o(\underline{r}, 0))}{\tau} + \frac{\rho_i}{\rho_E} \frac{H}{\tau} \quad (4)$$

in which $\tau = 4$ kyr is the assumed constant relaxation time of the adjustment process, $h_o(\underline{r}, 0)$ is the topography with respect

to sea level of the unglaciated state, ρ_i and ρ_E are the densities of ice and Earth respectively, and h' is the vertical bedrock deflection due to loading.

2.2. The Community Climate System Model (CCSM) of the US National Center for Atmospheric Research (v1.4)

This fully coupled atmosphere-ocean-sea ice-land surface processes model, the predictions of which we will compare to those of the ice-sheet coupled EBM, is the low resolution version of the CCSM described in Boville and Gent [1998]. This model consists of the above mentioned four independent components which are linked via a “flux coupler”. With the exception of the ocean, which communicates with the other three components on a daily basis, the three remaining components communicate hourly. The atmospheric component is referred to as the Community Climate Model (CCM) and is described by Kiehl *et al.* [1998]. For the purpose of the application of interest to us here this model will be run in paleoclimate mode at a spectral resolution of T31 in the horizontal which corresponds to a spatial resolution of ~ 3.75 degrees. The atmospheric model has 18 non-uniformly spaced levels in the vertical. Although this model includes the capability to separately account for the radiative effects of CO_2 , CH_4 , N_2O and chlorofluoro carbons, in the work to be described herein we will exercise only the CO_2 capability. The ocean component of the NCAR CCSM is the NCOM model described in detail in Gent *et al.* [1998], which has non-uniform horizontal and vertical resolutions which the authors refer to as $x3$ degree resolution. In the horizontal, the grid increases from 0.8 degrees latitude at the equator to 1.85 degrees latitude at the poles whereas it has a uniform 3.6 degree resolution in longitude. The vertical resolution is defined by 25 non-uniformly spaced levels in the radial direction with the shallowest (12 m deep) layer at the upper surface and the deepest (450 m deep) layer in the abyssal ocean. The ocean model employs the eddy mixing parameterization of Gent and McWilliams [1990] and Gent *et al.* [1995] in the horizontal tracer equations but the non-local K-profile boundary layer mixing parameterization of Large *et al.* [1994], with a background value of the mixing coefficient of $1.5 \times 10^{-5} \text{ m}^2/\text{s}$, is employed in the vertical. The sea ice component of the CCSM is the model of Weatherly *et al.* [1998] which consists of the three layer thermodynamic component of Semtner [1976] and the dynamical component of Flato and Hibber [1992]. Because this version of the model has no river run-off scheme, in order to ensure conservation of fresh water it continuously computes the net evaporation from the active (i.e. non sea ice covered) surface of the ocean as well as the net precipitation onto the active surface of the ocean, and then simply augments the net precipitation onto the active surface of the ocean so as to ensure conservation of the mean salinity.

This version of the CCSM has recently been subjected to a significant test by employing it to simulate the climate of Last Glacial Maximum [Peltier and Solheim, 2003]. For the purpose of this test the model was initialized under modern conditions of both the circulations of the atmosphere and oceans but with LGM surface, trace gas and insolation forcing conditions applied. It was then integrated forward in time until statistical equilibrium was fully achieved. The results for a variety of properties of LGM climate were then compared with paleoceanographic inferences, including the differential strength of the North Atlantic thermohaline circulation under modern and LGM conditions, the differential in sea surface temperatures across the tropics and the differential strength of El Niño. As discussed in detail in Peltier and Solheim [2004], the results of these analyses are the first to have provided full agreement with paleoceanographic observations, especially in regards to the strength of the Atlantic THC at Last Glacial Maximum.

2.3. Design of the Numerical Experiments Concerning the Neoproterozoic Snowball Glaciations

Insofar as our experiments with the ice-sheet coupled EBM are concerned, we will make use of the high numerical efficiency of this model to explore the range of steady-state surface climates that are expected to arise under variations of the concentration of atmosphere $p\text{CO}_2$. For the purpose of all of these experiments we will assume, as in Hyde *et al.* [2000], that the continental configuration is one which approximates the distribution that is expected to have obtained during the most recent (Veranger/Marinoan) event in the interval from ~620 Ma to ~580 Ma. The continental reconstruction of Dalziel [1997] for 545 Ma will be employed as an approximation to the Marinoan distribution, the main characteristic of which is that the remaining main mass of Rodinia was then located in a predominantly south polar location. This interpretation of the available paleomagnetic constraints is somewhat consistent with that in Eyles and Januszczak [2003] (see their Figure 4b) although the latter authors have assumed a higher degree of tropical continentality to have existed at this time. All of the experiments using the ice sheet coupled EBM will be performed assuming a 6% reduction in the solar constant (unless otherwise indicated) and an orbital geometry the same as modern. Furthermore, no account will be taken of the change in the length of the day that is inferred to have been characteristic of this time in the past. The latter issue should not be a cause for concern with respect to the simulations with the ice sheet coupled EBM but could be of interest in regards to the results obtained using the NCAR CCSM.

For the purpose of the experiment to be described using this more complete model of the climate system we will employ the same continental distribution and 6% decrease of

the solar constant and will start with a continental ice cover distribution equal to that predicted using the ice-sheet coupled EBM at an atmospheric $p\text{CO}_2$ equal to modern. The model will then be integrated forward in fully coupled mode (spun-up) until statistical equilibrium is achieved. This will allow us to test the validity of the prediction of the simple model, which includes no influence of ocean dynamics, when ocean dynamics are included, when precipitation and evaporation are computed in a self-consistent manner, and when the sea ice model includes not only thermodynamics but also dynamics. For the purpose of these complex integrations, an initial discussion of which appeared in Peltier [2002], the bathymetric depth of the oceans will be taken to be a constant 4000 m everywhere. As we will see, the integration of this model from a warm state into statistical equilibrium will require an integration time of approximately 425 years.

3. RESULTS FROM THE EBM/ISM AND CCSM EXPERIMENTS

Although the two models described in the previous Section of this paper are dramatically different insofar as their level of complexity is concerned, as we will see their predictions of Neoproterozoic equilibrium climate are somewhat similar.

3.1. Neoproterozoic Equilibrium Climates from the EBM/ISM and the Possible Existence of a “ CO_2 Attractor”

A primary result of this paper is that shown in Figure 2 which plots the mean sea level temperature over the surface of the Earth as a function of the deviation, in Watts per square meter, of the surface radiation balance due to a decrease or increase in atmospheric $p\text{CO}_2$. If C_o is the modern atmospheric concentration of CO_2 and C is the modified concentration, then the quantity $d\text{Rad}$ (W/m^2), which is the change in the surface radiative forcing due to the change in CO_2 concentration from C_o to C , is such that (see IPCC WG-1, 1996):

$$d\text{Rad} = 5.35 \times \ln \left[\frac{C}{C_o} \right]. \quad (5)$$

For $C = 2 C_o$ this gives $d\text{Rad} \cong 4 \text{ W}/\text{m}^2$. This is consistent with the results of Ramanathan *et al.* [1979] and can be re-expressed [see Tarasov and Peltier, 1999, equation (3)] as a perturbation (ΔA) to the parameter A in equation (1), in the form:

$$\Delta A = k \ln \left[\frac{C}{C_o} \right]. \quad (6)$$

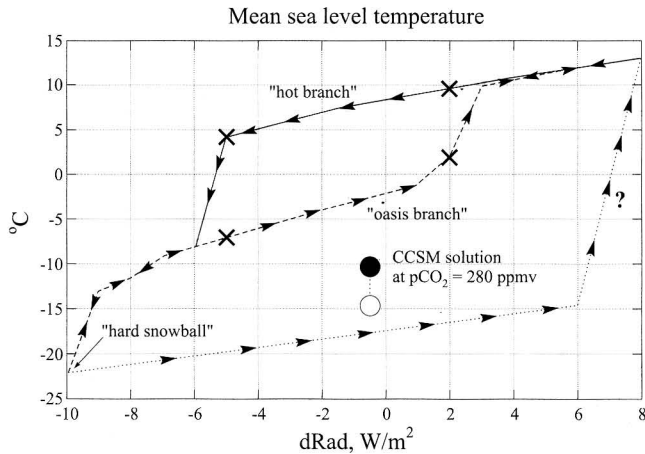


Figure 2. Mean sea level temperature as a function of atmospheric carbon dioxide concentration according to the ice sheet coupled energy balance model that has been developed at the University of Toronto. For the purpose of the computation of the large number of steady-state solutions that define the individual segments of this diagram it has been assumed that the solar constant was reduced by 6% below modern and that the parameters A and B in equation (1) that define the infrared contribution to the surface climate forcing remain fixed to modern climate values (see the text for a discussion of the implication of this assumption). The co-albedo of sea ice has been assumed to be equal to 0.55. Also shown on this Figure as the solid black circle is the mean sea level temperature solution delivered by the NCAR CCSM for an atmospheric CO_2 concentration of 280 ppmv, the continents fully glaciated and the same 6% reduction of the solar constant assumed in the integrations of the simpler model employed to construct the state-space diagram. The open circle is the result for mean surface temperature delivered by the NCAR CCSM prior to reduction of the data to sea level.

For the purpose of the results to be presented herein, we will express the changes to the surface radiation balance due to changes in atmospheric pCO_2 simply in terms of $d\text{Rad}$. The implied concentration of CO_2 is then simply inferable by inverting (5), recognizing that the constant factor 5.35 in (5) or k in (6) may be different under Neoproterozoic conditions than it is under modern conditions. This point will turn out to be important to the understanding of the results of our analyses. Specifically it will be important to understand that when we compare climate states for different concentrations of CO_2 , computed using the EBM/ISM, with those obtained for the same concentration of CO_2 using the NCAR CCSM, we should not expect to obtain precisely the same climate, even when both models are driven by a solar forcing that is 6% lower than modern. The reason for this is that the more complete model not only includes the direct effect on climate due to the change in atmospheric pCO_2 but also the indirect effect due to the fact that in the colder climate that obtains with the 6% reduction of the solar constant, there is a marked decrease in the water vapour

concentration in the atmosphere and therefore a significantly further enhanced modification to the greenhouse effect.

Inspection of Figure 2 will demonstrate that the ice sheet coupled EBM exhibits hysteresis in the mean sea level temperature as a function of $d\text{Rad}$ (note that positive values of $d\text{Rad}$ indicate CO_2 concentrations higher than modern, where the modern value is taken to be equal to 300 ppmv, whereas negative values indicate decreases). For the standard values of the model parameters (mean annual precipitation rate = 0.6 m yr^{-1} , solar constant reduced by 6% from modern, sea ice co-albedo = 0.55, continental freeboard = 400 m), the region of hysteresis exists in the range $d\text{Rad} = -6 \text{ W/m}^2$ to $d\text{Rad} = +3 \text{ W/m}^2$, on which mean sea level temperatures vary between -8°C and $+10^\circ\text{C}$. This hysteresis curve for the University of Toronto EBM coupled ice sheet model is very similar to that described in *Crowley et al.* [2001] using an earlier version of the model described in *Deblonde et al.* [1992] in which the ice sheet component of the model was assumed to be isothermal. As denoted on the Figure, the cold segment of the hysteresis loop will be referred to as comprising the “oasis branch” of solutions. We will refer to the upper branch of the hysteresis loop as the “hot branch”. Also shown on this Figure, in the vicinity of $d\text{Rad} = -10 \text{ W/m}^2$, are solutions for which the mean surface temperature is less than -20°C . These are the “hard snowball” solutions called upon qualitatively by *Kirschvink* [1994] as a possible explanation for the intense low latitude glaciations that are supposed to have occurred during the Neoproterozoic. Also drawn on this Figure is a third branch of solutions that extend from $d\text{Rad} = -10 \text{ W/m}^2$ to $d\text{Rad} = +6 \text{ W/m}^2$ which is rather flat but which, for $d\text{Rad}$ between $+6 \text{ W/m}^2$ and $d\text{Rad} = +8 \text{ W/m}^2$, rises rapidly to reconnect with the extension to the “hot branch” of solutions. The arrows on this plot of steady-state solutions to the ice sheet coupled EBM indicate the route or routes by which climate states on the various branches of the diagram may be accessed. States on the “hot branch” of the hysteresis loop may be accessed only by cooling (by diminishing $d\text{Rad}$) from states at higher temperature or by warming from an adjacent state on the hot branch. On the other hand states on the “oasis branch” of the hysteresis loop may only be accessed by warming from “pre-hard-snowball” cold states along the portion of the diagram in the range $-10 \text{ W/m}^2 < d\text{Rad} < -6 \text{ W/m}^2$. Points on the hot branch cannot be accessed by warming from states in this range. Once a “hard snowball” climate has been achieved for $d\text{Rad} < -10 \text{ W/m}^2$, the only way to escape is by increasing $d\text{Rad}$ such that $d\text{Rad} > 8 \text{ W/m}^2$. The precise value of the CO_2 increase required to escape the “hard snowball” state is not accurately determined by this model as it does not include a detailed calculation of the influence of the thickness of the sea ice layer that must be eliminated before the system can escape its deeply frozen state. *Hoffman and Schrag* [2002]

accept that escape would require an increase of CO_2 concentration to as much as 1000 times modern and suggest that this would be produced by the action of volcanism, citing the sometimes observed “cap carbonates” as evidence for the occurrence of rapid draw-down of CO_2 into the ocean that would have occurred once the global sea ice cover was eliminated. If this degassing flux were to have been equal to modern it is estimated that several million years would be required for this escape event to occur. It is important to note, a fact not discussed in *Crowley et al.* [2001], that the oasis solutions appear only in circumstances in which ice-fluxes large enough to force early glaciation occur. We find that when a standard explicit elevation-desert feedback is introduced then no hysteresis loop forms—oasis solutions do not arise. Although this paper is based upon an exploration of the implications of the existence of hysteresis, it is therefore an open issue as to whether this actually occurs in nature.

Plate 2 shows surface temperature distributions for the 4 points marked on the hysteresis curve of Plate 1. Both oasis and non-oasis solutions are shown for $d\text{Rad} = -5 \text{ W/m}^2$ and for $d\text{Rad} = +2 \text{ W/m}^2$. The non-oasis solution at $d\text{Rad} = +2 \text{ W/m}^2$ has a continental ice-sheet that is confined to the polar portion of the southern hemisphere supercontinent and a small sea ice cap covering the northern hemisphere polar ocean. At $d\text{Rad} = -5 \text{ W/m}^2$ the continental ice sheet at the south pole expands significantly as does the polar cap of northern hemisphere sea ice, but the latter only slightly. On the oasis branch at $+2 \text{ W/m}^2$, on the other hand, the southern hemisphere supercontinent is fully glaciated, even in equatorial latitudes, and the north polar cap of sea ice has shifted to lower latitudes. At $d\text{Rad} = -5 \text{ W/m}^2$ on the oasis branch sea ice extends from the north pole and connects to the glaciated southern hemisphere supercontinent but an oasis of open water continues to persist at the equator. Climate states in the range $-10 \text{ W/m}^2 < d\text{Rad} < -6 \text{ W/m}^2$ are all of oasis form, therefore suggesting from equation (5), that oasis solutions should persist down to atmospheric CO_2 concentrations as little as $\sim 40 \text{ ppmv}$. To the extent that this ice sheet coupled EBM is an adequate representation of Neoproterozoic climate during the Veranger/Marinoan event, therefore, it is clearly incumbent upon the proponents of the hard snowball Earth scenario to provide a believable mechanism whereby the required decrease of atmospheric $p\text{CO}_2$ might have been produced. Although one or two suggestions of possibilities have been made in the literature, these must at present be seen as somewhat fanciful.

Plate 3 shows the results of a number of sensitivity analyses of the stability of the Neoproterozoic hysteresis loop to changes in the parameters of the base model. On the top portion of this Plate we have superimposed such loops for several variations on these parameters. Inspection will show that decreasing the annual precipitation rate from 0.6 m/yr to 0.3

m/yr shifts the centroid of the loop to a lower value of $d\text{Rad}$ ($\text{preco} = 0.3$). Similarly, a 20% increase in the latitude dependent thermal diffusion coefficient $D(\theta)$ ($D_{\text{fac}} = 1.2$) shifts the loop to lower $d\text{Rad}$ whereas a similar decrease $D_{\text{fac}} = 0.8$) has a slight but opposite effect. The largest influences registered on this diagram, however, are those due to changes in the extent to which the solar constant has been reduced. If, instead of the 6% reduction assumed in the base model, we assume a 7% reduction ($Q_{\text{fac}} = 0.93$), then the hysteresis loop is shifted to higher $d\text{Rad}$. On the contrary, if the reduction of the solar constant is only 5%, the loop is similarly shifted to lower values of $d\text{Rad}$. These results imply that, during the Neoproterozoic, the region of hysteresis may exist for $-9 \text{ W/m}^2 < d\text{Rad} < +5 \text{ W/m}^2$. The lower plate of Figure 2 shows “blow-ups” of the oasis branch of solutions on which the low $d\text{Rad}$ corners of the hysteresis loops are denoted by a square symbol.

3.2. A Simulation of the Climate of the Neoproterozoic Period Using the NCAR CCSM

It is prohibitively expensive of computer resources to attempt to reproduce the hysteresis loop shown on Plate 1 using a fully articulated climate model such as the NCAR CCSM. This will be clear on the basis of the analysis of LGM climate described in *Peltier and Solheim* [2004] in which it is shown that integration of the model to statistical equilibrium required a simulation in excess of 2000 calendar years duration. Although the continuing increase of CPU speed of commercially available computing systems will eventually make it possible to compute the equivalent hysteresis loop (if it exists!) for the complete CCSM, for present purposes we will content ourselves with describing a single run of the model to statistical equilibrium from a warm initial state at an atmospheric CO_2 concentration equal to preindustrial (280 ppmv), with the solar constant reduced by 6% and for the same continental configuration as that employed to compute the solutions for the ice sheet coupled energy balance model described in the last subsection. However, we will also assume that the continental ice cover at this CO_2 level is equal to that which obtains on the oasis branch of solutions of the simpler model. In this way we will be able to test the issue as to whether the equilibrium climate of the CCSM delivers a mean sea level temperature that is close to that predicted by the EBM/ISM. This may be construed to constitute a preliminary test of whether or not the same hysteresis loop might exist in the solution space of the NCAR model and whether or not the same refugium solutions exist in the full climate model as exist in the solution space of the EBM/ISM.

Figure 3 shows the results obtained for the spin-up period of the integration of the CCSM in terms of a number of global properties of the climate system that are diagnostic of climate

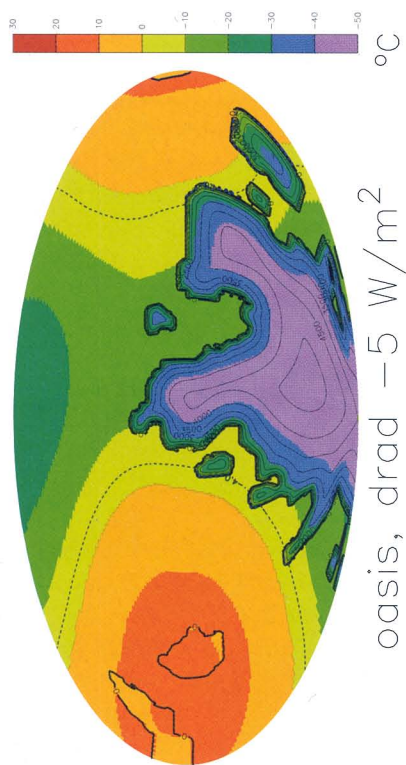
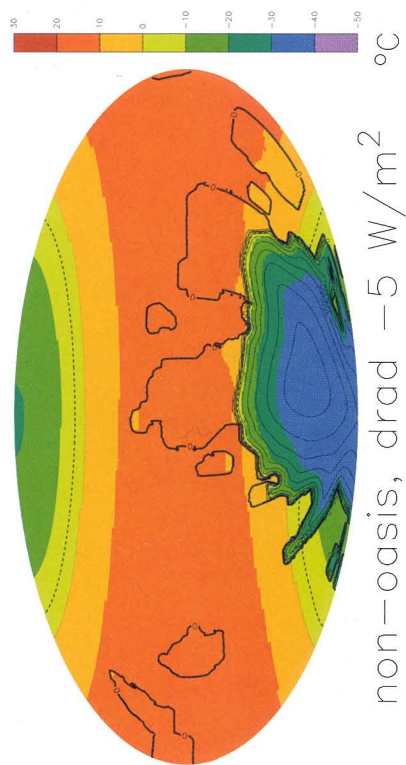
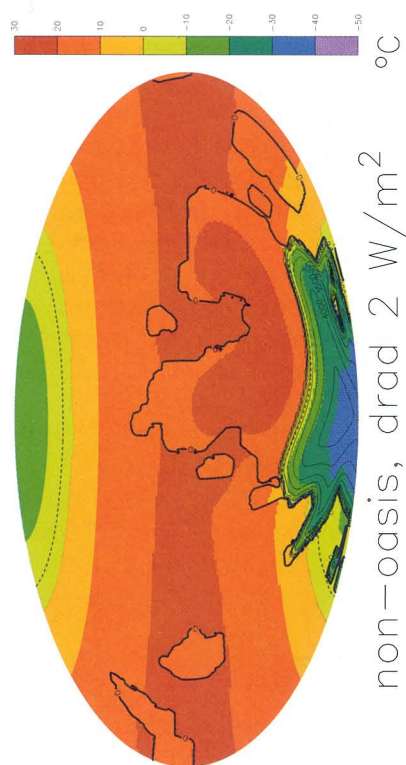
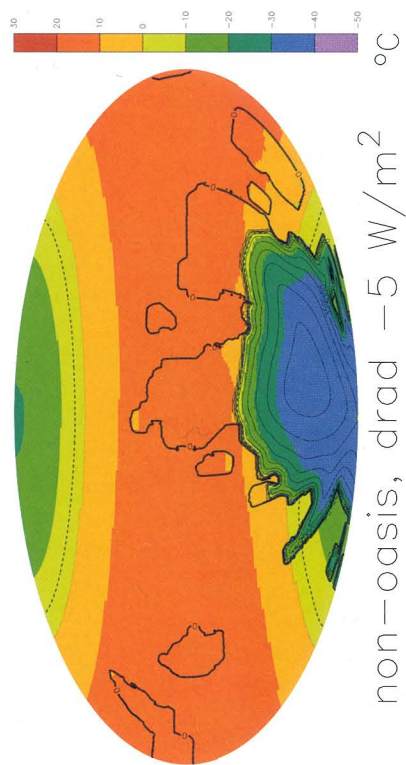


Plate 2. Surface temperature fields for the four steady-state solutions of the EBM/ISM at the points on the hysteresis curve of Figure 2 denoted by the symbol x . Also shown on each of these plots of sea level temperature is the zero degree Centigrade line, shown dashed, which encloses the regions that are covered by sea ice. The extended continental glaciation is also clearly depicted together with the topography contours over the land-ice covered regions:

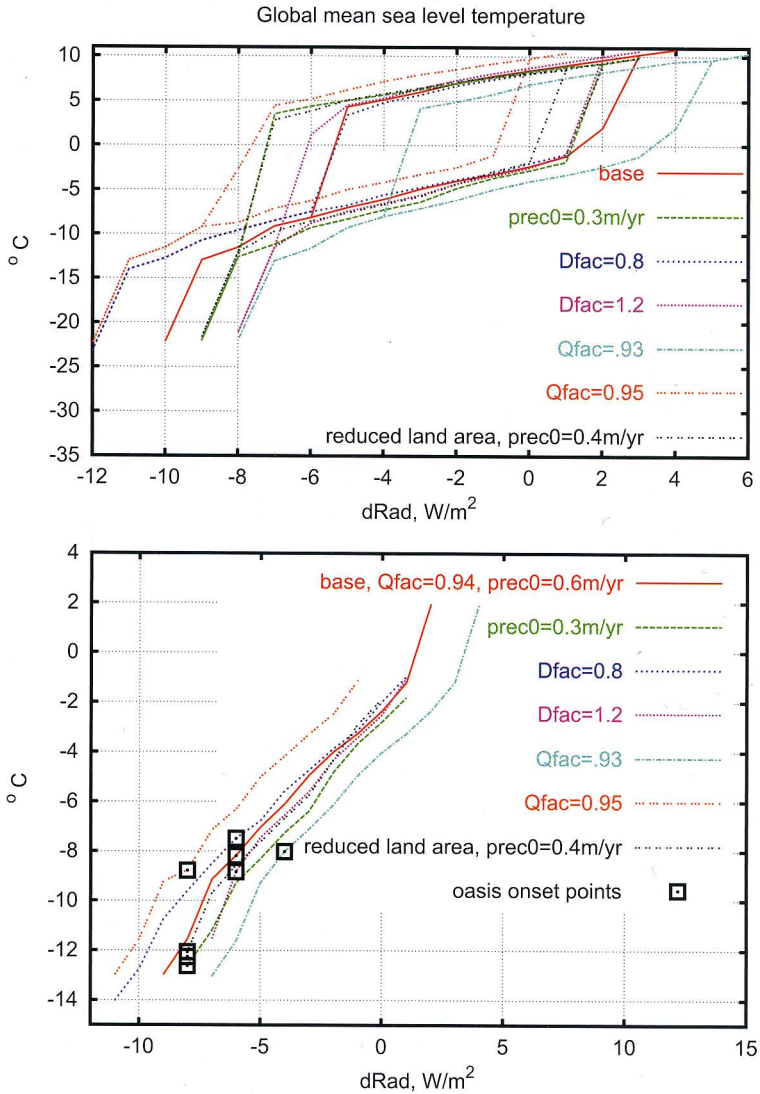


Plate 3. (Top Frame) The hysteresis loops delivered by the EBM/ISM with variations of the parameters of the base model shown on the key. (Bottom Frame) Blow up of the “oasis” branch of the hysteresis curves shown in the Top Frame with the low temperature corner of this branch indicated by the square symbol.

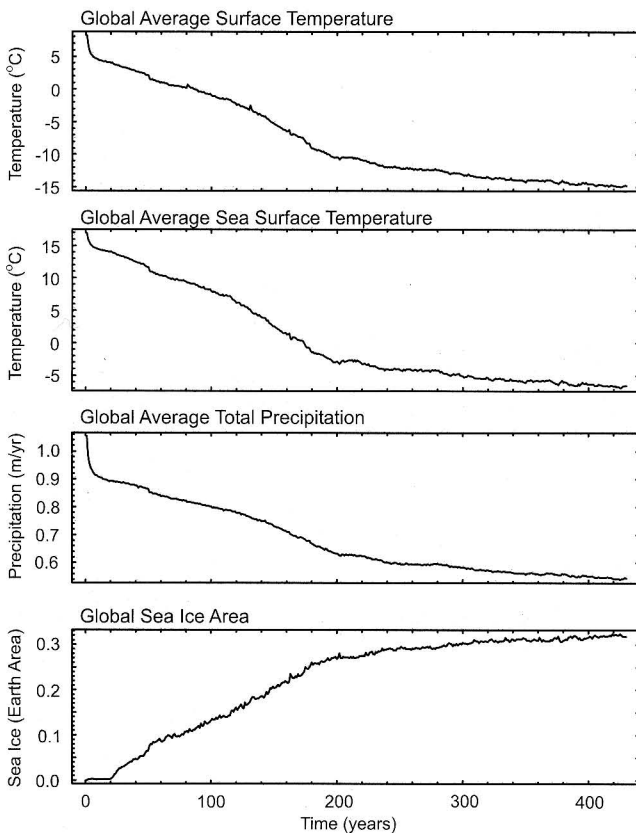


Figure 3. Spin-up to equilibrium data from the 425 year run of the NCAR CCSM for the climate of the Neoproterozoic using the same continental configuration as that employed with the EMB/ISM and the same 6% reduction of the solar constant. For the purpose of this integration the atmospheric CO_2 concentration has been fixed at the modern pre-industrial level of 280 ppmv and the continents have been assumed to be fully glaciated. Spin-up data are shown for annual and global mean surface temperature, annual and global mean sea surface temperature, annual and global mean precipitation and annually averaged sea ice area. All of these data have also been averaged for the last 50 years of model integration, a period during which the system appears to be close to statistical equilibrium.

state, including the globally averaged surface temperature, the globally averaged sea surface temperature, the globally averaged precipitation rate and the total area of sea ice cover. Inspection of the Figure will show that statistical equilibrium of the model climate has been essentially achieved after approximately 425 years of simulated evolution. That the spin-up time for the Neoproterozoic integration should be less than was required for the LGM integration of *Peltier and Solheim* [2004] is unsurprising since the geometry of the ocean basins is considerably simpler so that the complexity of the thermohaline circulation is considerably diminished. Aside from the number of simulated years required to reach a state of approximate statistical equilibrium it is important to note that the

average precipitation rate that is characteristic of this eventual equilibrium is very close to the 0.6 m/yr value assumed in the integrations performed of the EBM/ISM for which results were shown on Figure 2 (Note, however, that the choice $\text{preco}=0.3 \text{ myr}^{-1}$ in the EMB/ISM gives a result that is closer to the CCSM global mean precipitation of 0.6 m yr^{-1} because of the power law dependence of $\text{prec}(t)$ discussed in Section 2.1). It is also important to note from the final frame on Figure 3 which shows the variation with time of the area covered by sea ice, that this property of the Neoproterozoic climate state is also close to equilibration, implying that a hard snowball state will not form in a climate in which the concentration of atmospheric CO_2 is equal to the modern preindustrial level. Because the system does continue to drift very slowly towards a colder equilibrium, however, we cannot be entirely sure that a further diminution of the area of the open water refugium would not occur if the system were integrated further forward in time.

Of equal importance from the perspective of the analyses reported herein, to that demonstrating the quasi-equilibrium of the area covered by sea ice, is the quasi-equilibrium result for the globally averaged surface temperature. The equilibrated value of mean surface temperature produced by the CCSM is -14.8°C , a value which, when corrected for the topography of the ice covered continents, reduces to a mean sea level temperature of -10.3°C . The former and latter values are plotted on Figure 2 as the open circle and solid circle respectively. Inspection of this result from the CCSM relative to the result for the equivalent point on the oasis branch of the hysteresis loop delivered by the EBM/ISM, which corresponds to a value of $\Delta A = -0.41 \text{ W/m}^2$ at $[\text{CO}_2] = 280 \text{ ppmv}$, will show that the mean sea level temperature of the equilibrium predicted by the CCSM is more than 5°C colder than that delivered by the EBM/ISM. As previously mentioned this is an entirely expected consequence of the fact that the parameters A and B employed in the representation of the infrared forcing in the simple model have not been re-calibrated so as to properly represent Neoproterozoic conditions which are characterized by a significant reduction of the IR contribution due to water vapour feedback.

Of primary interest for present purposes, however, is the nature of the equilibrium solution that the CCSM has delivered. This equilibrium is illustrated in Plate 4 on which we show, in Mollewieide projection as for Plate 2, the 50 year averaged equilibrium fields for annually averaged surface temperature, annually averaged sea surface temperature, annually averaged precipitation rate and annually averaged sea ice cover. Focusing first upon the latter field and comparing it to the results for various points on the hysteresis curve of Figure 2, it will be clear that the CCSM result is for an oasis solution that is most like the EBM/ISM result on the oasis

branch for $dRad = -5 \text{ W/m}^2$ although there is no sea ice connection to the south polar supercontinent as there is in the EBM/ISM result. Inspection of the remaining frames of Plate 4 simply illustrates the further properties of the climate that characterizes the oasis solution delivered by the CCSM. Of special note is the relatively high rate of precipitation that continues to occur along the intertropical convergence zone and the still rather warm SSTs with temperatures in excess of 15°C characteristic of this same region.

Although space will not allow us to provide a discussion of the full range of diagnostic analyses that relate to the detailed characteristics of the circulations of the atmosphere and ocean in this simulation, it proves interesting by way of summary to show some degree of further detail. To this end Plate 5 shows, in the upper and lower frames respectively, the properties of the annually averaged surface pressure and wind fields over the surface of the planet and the overturning circulation of the ocean represented by the zonally averaged meridional transport stream function. The former frame reveals strong tropical easterlies in the equatorial region over the ocean and intense midlatitude westerlies in approximate (quasi-) geostrophic balance with the surface pressure field. The nature of the overturning circulation of the oceans according to this model result is especially interesting. The lower plate of Plate 5 demonstrates this to be governed by intense mid latitude sinking in the northern hemisphere to the south of the sea ice cap and somewhat weaker sinking around the coast of the ice-covered southern hemisphere supercontinent. It appears to be the strong sinking due to brine rejection along the sea ice front which draws warm equatorial water northwards and thereby strongly inhibits the southerly extension of the northern hemisphere sea ice cap which is required in order for the system to descend into the hard snowball state. As previously discussed in *Peltier* [2002], therefore, the influence of ocean dynamics is such as to significantly inhibit the occurrence of the snowball bifurcation. Although deep water also forms along the coast of the glaciated southern hemisphere supercontinent, as it does today around Antarctica, the water mass that is formed by this process is not nearly as influential as that which forms due to sinking in the north although it also serves to impede sea ice advance by warming this southern region and drawing warm equatorial water southwards.

4. A “CO₂ ATTRACTOR” IN THE NEOPROTEROZOIC

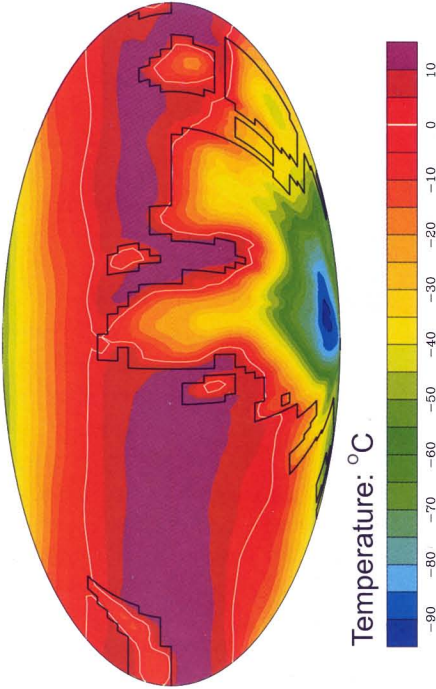
In attempting to bring together the observational evidence for the large amplitude oscillations in $\delta^{13}\text{C}$ that are characteristic of the Neoproterozoic era and the results of the simulations of the physical climate system discussed in the last Section of this paper, we seek a mechanism or mechanisms that would strongly couple the physics to the biogeochemistry.

Clearly the possible existence of hysteresis in Neoproterozoic climate evidenced in Figure 2 is highly suggestive of the possibility of the existence of a “CO₂ Attractor” as speculated upon recently in *Crowley et al.* [2001]. Their idea was simply as follows, although no attempt was made in that paper to articulate it in any detail. Suppose, for some reason, the CO₂ concentration in the atmosphere is decreasing and the system is in an initial state on the “hot branch” of the hysteresis loop in Figure 2. Eventually, as CO₂ levels continue to fall, the system will experience the sharp decrease in temperature that is precursory to its final descent into the hard snowball state. Suppose furthermore that some physical/biogeochemical process were to come into play, once the system descends from the “hot branch”, which strongly opposes the continuing CO₂ decrease and in fact acts such as to reverse this initial tendency. The system would then warm along the oasis branch until finally it executes the rapid warming that takes it back onto the hot branch. If the same process that originally inhibits the descent onto the hard snowball state were then to inhibit its further ascent along the hot branch, we would have the possibility of an oscillatory system in which the atmospheric concentration of CO₂ would oscillate between the extrema that define the low concentration and high concentration edges of the hysteresis loop, simply going around the loop again and again until some additional process acts so as to allow it to escape.

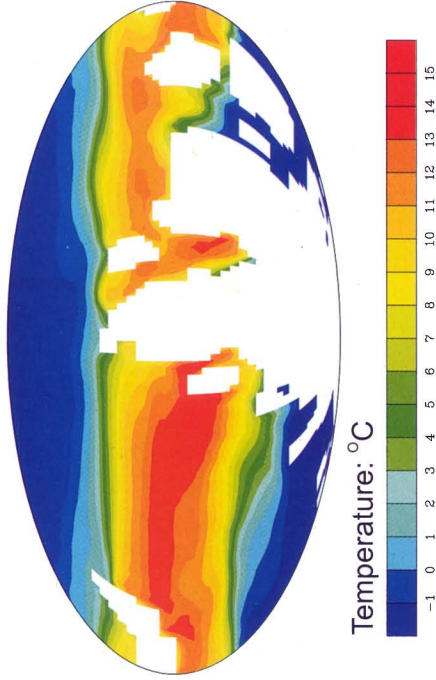
What remains to be understood, if this hypothesized behaviour is to be realized, is the nature of the nonlinear process whereby entrapment onto the hysteresis loop is forced to occur. If we were able to identify such a mechanism, then we might associate the large amplitude $\delta^{13}\text{C}$ oscillations shown on Plate 1 with a limit cycle solution of a nonlinear system that included this mechanism as well as the elements of the physical climate system that support the existence of the hysteresis loop.

One suggestion of what this mechanism might involve has very recently been discussed by *Rothman et al.* [2003] although the authors were apparently unaware of the paper of *Crowley et al.* [2001] in which the idea of a Neoproterozoic “CO₂ Attractor” was first suggested. It will therefore be useful to discuss the idea of Rothman et al. in the context of the present analysis. Rothman et al. provide a very compelling argument to the effect that the oscillations of $\delta^{13}\text{C}$ that occurred during the Neoproterozoic cannot be explained by a conventional model of the carbon cycle in which equilibrium is assumed to exist between the interacting reservoirs of organic carbon and inorganic (carbonate) carbon (which includes all of the CO₂ dissolved in the oceans and all of the CO₂ in the atmosphere). They trace the necessarily disequilibrium dynamics of the Neoproterozoic interval to the existence of an extremely massive organic carbon reservoir confined to the oceans. This reservoir during the Neoproterozoic is argued to have con-

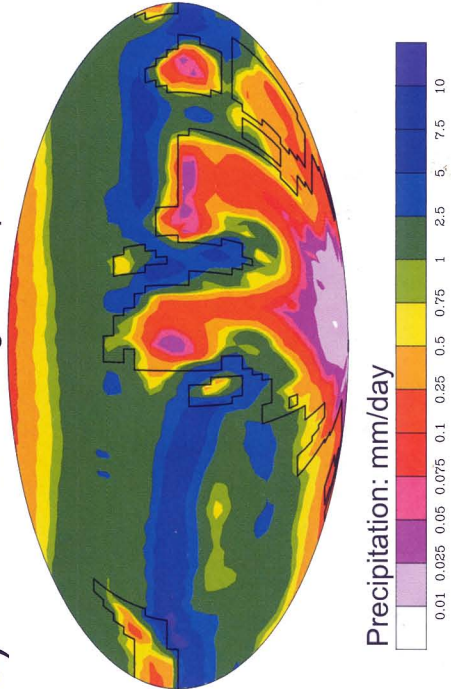
a) Annual Average Surface Temperature



c) Annual Average Sea Surface Temperature



b) Annual Average Precipitation



d) Annual Average Sea Ice Cover

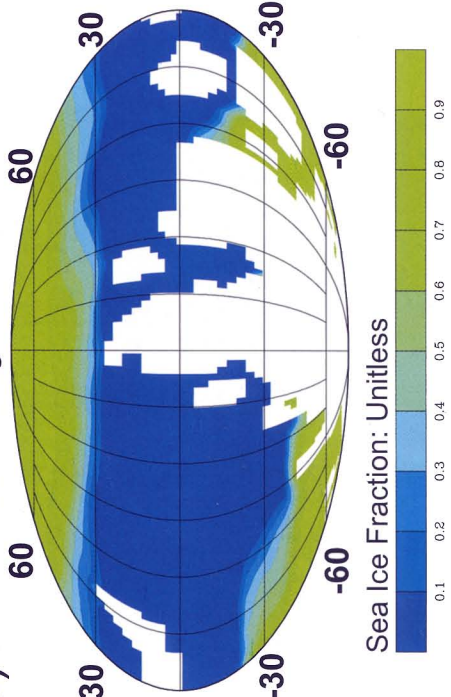
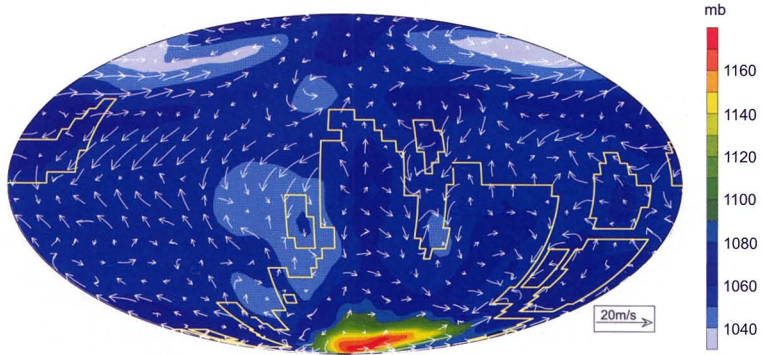


Plate 4. 50 year averaged fields for surface temperature, sea surface temperature, precipitation and sea ice area from the end of the Neoproterozoic integration.

Surface Winds and Mean Sea Level Pressure



Global Meridional Transport Streamfunction

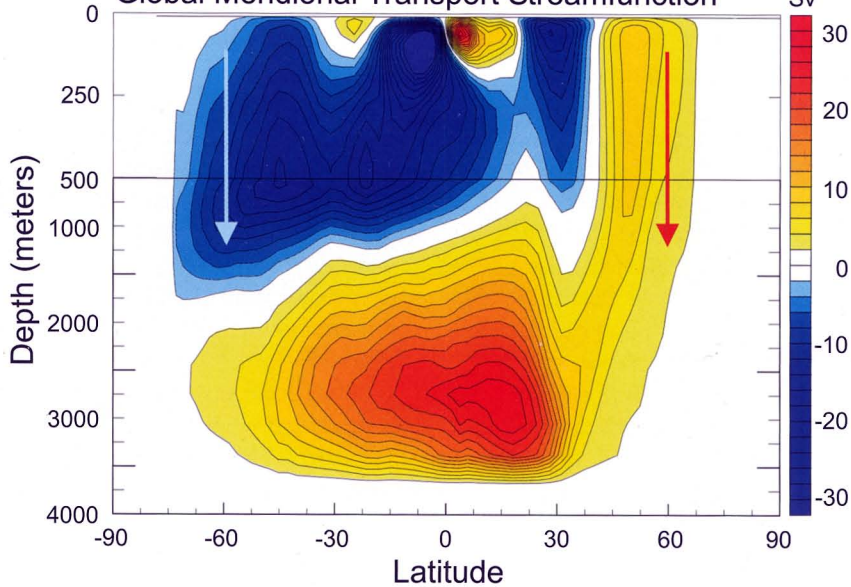


Plate 5. (Top) Surface pressure and wind field annually averaged and averaged over the last 50 years of Neoproterozoic model evolution. (Bottom) The meridional overturning streamfunction of the oceans from a 50 year and annually averaged data set from the Neoproterozoic integration.

tained as much as 100 times the organic carbon as do the present day oceans. Figure 4, which is reproduced from their paper, illustrates the 2 box model of the carbon cycle that the authors employ as basis for their analysis. In this diagram δ_1 and τ_1 are the isotopic contents and residence times in the inorganic reservoir and δ_2 and τ_2 those for the organic reservoir. Rothman et al. show that $\tau_2 \gg \tau_1$ is consistent with the out of equilibrium behavior required by the observed relationship between the isotopic composition of carbonate and the difference between the isotopic compositions of carbonate and organic carbon. They show by computation on an explicit mathematical model (their equations 6–9) of the interacting reservoirs that the carbon cycle model under these conditions is able to deliver an excellent facsimile of both the positive and negative phases of the $\delta^{13}\text{C}$ oscillations shown on Plate 1.

The most interesting aspect of their analysis, however, concerns a brief speculation as to how descent into a snowball glaciation event may be arrested so as to prevent entry into the hard snowball state and thereby require that the coldest achievable states are those of the oasis type first identified by Hyde et al. [2000], whose work Rothman et al. reference in this connection. Rothman et al. point out that as the ocean cools as a consequence of a shift to lower levels of atmospheric CO_2 concentration, “more O_2 would be partitioned into the ocean in a colder climate”. As the ocean becomes more strongly ventilated the organic carbon reservoir would become re-mineralized thereby increasing the amount of CO_2 in the carbonate reservoir. They argue that this effect would be extremely important because the solubility of O_2 in sea water increases by a factor of 2 as the water temperature drops from 30°C to 0°C . If we now connect this biogeochemical effect to the physical hysteresis loop shown in Figure 2, then we clearly have the basis for the existence of the nonlinear limit cycle behavior required to understand the $\delta^{13}\text{C}$ oscillations shown on Plate 1. As the system descends to lower values of atmospheric CO_2 concentration along the hot branch of the hysteresis loop,

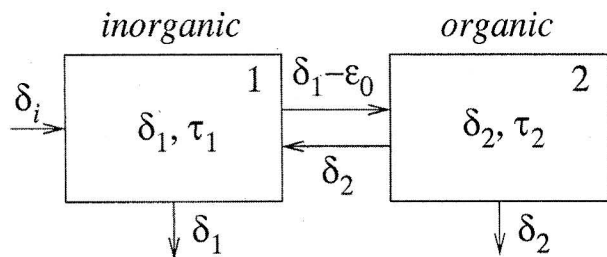


Figure 4. The 2 box model of the carbon cycle employed in the analysis of Rothman et al. [2003]. The box of isotopic composition δ_1 and residence time τ_1 denotes the carbonate box whereas the box of isotopic composition δ_2 and residence time τ_2 denotes the organic carbon box. When carbonate (CO_2) is transformed to organic carbon through photosynthesis an isotopic fractionation ϵ_0 occurs.

eventually the system cools sufficiently that the draw down of O_2 from the atmosphere into the ocean results in the remineralization of the organic reservoir and the CO_2 concentration begins to rise again, but now along the oasis branch of the hysteresis loop of Figure 2. Eventually the system warms sufficiently as to cause it to execute the jump from the oasis branch to the hot branch. This warming exhausts the oxygen from the ocean, thereby decreasing the rate of remineralization of the organic reservoir, thereby causing the atmospheric concentration of CO_2 to begin to decrease once more. The origin of the $\delta^{13}\text{C}$ oscillations shown on Plate 1 is thereby explained by combining the fact that there is hysteresis in the physical climate system to variation of the concentration of atmospheric CO_2 , together with the potential for strong negative feedback (the restoring force required to support an oscillation) due to the O_2 mediated biogeochemistry. That this suggestion is plausible follows from the fact that increased remineralization of (light) organic carbon both lowers $\delta^{13}\text{C}$ and increases $p\text{CO}_2$, provided that the dynamical condition identified in Rothman et al. [2003] is met.

Of course this model works only to the extent that the atmospheric concentration of O_2 was high enough during the Neoproterozoic to serve as the required link between the physical and biogeochemical components of the system. Rothman et al. [2003] provide an estimate of this requirement that suggest that a level that is only 4% of the present atmospheric O_2 concentration would be sufficient. In this regard it would appear that the early paper of Broecker [1970] is crucial to the success of the argument that we are presenting herein. Broecker’s paper deals explicitly with the linkage between the organic and inorganic carbon reservoirs and the importance of the atmospheric oxygen concentration to this inter-connection. This idea is well captured in the following sentences which we quote directly from this paper. “The enrichment of ^{13}C in the carbonate carbon that necessarily accompanied the growth of the organic reservoir must have resulted in a shift in the $^{13}\text{C}/^{12}\text{C}$ ratios in sea water. This shift should be recorded in marine carbonates formed in the course of this transition period. Therefore, the absence of such a shift in the $^{13}\text{C}/^{12}\text{C}$ ratio in carbonates deposited from early Paleozoic to recent time [Craig, 1953; Keith and Webber, 1964] implies that the development of the organic carbon reservoir, and hence of the atmospheric O_2 reservoir, occurred prior to Paleozoic time”. Here Broecker is clearly using the deep interconnection of O_2 to the two primary reservoirs, whose interaction constitutes the carbon cycle, to argue that the concentration of atmospheric O_2 must have been high early in Earth history, but the interaction he invokes is precisely that called upon in the Rothman et al. [2003] paper. In this scenario the hard snowball glaciations of Hoffman and colleagues are impossible to achieve. Rather, the coldest climate states that are realizable are those of “oasis” type which lie

along the cold branch of the hysteresis curve in Figure 2. Even if it were to turn out that the strong hysteresis effect that we have identified herein were found not to occur in the climate system of the Earth, it may nevertheless prove possible for a strongly nonlinear oscillation of $\delta^{13}\text{C}$ to exist as a consequence of the feedbacks we are discussing.

5. CONCLUSIONS

The arguments presented herein are clearly in an early stage of development and there are several outstanding issues that will have to be resolved before we will be in a position to suggest that our hypothesis concerning the nature of Neoproterozoic glaciation is entirely sound. Among these outstanding issues, one that may be especially critical concerns the fundamental question as to whether hysteresis actually exists in a more complete climate model than that consisting of the ice sheet coupled energy balance model for which we have established it herein. In the absence of the detailed analyses that will be required to demonstrate the existence of multiple equilibria in the more complete model, the absence of this necessary analysis must stand as a caveat upon the hypothesis that we have advanced herein. If we are successful in establishing the existence of hysteresis in the fully coupled model, it will be important to extend the simpler ice sheet coupled EBM so as to explicitly incorporate the carbon cycle model of Rothman *et al.* [2003] together with the mediating influence of atmospheric O_2 as originally discussed in Broecker [1970]. It would appear that a biogeochemistry coupled model of the physical climate system of this kind would constitute an interesting vehicle with which to further explore the fascinating issues in Earth evolution that surround the problem of the Neoproterozoic carbon cycle.

Acknowledgments. This paper is a contribution to the Climate System History and Dynamics Programme that is sponsored by the Natural Sciences and Engineering Research Council of Canada and by the Meteorological Service of Canada. The work has also been supported by NSERC Grant A9627. Very helpful reviews of the first draft of this paper were provided by Dan Rothman and a second (anonymous) referee. We are grateful to them both.

REFERENCES

- Agassiz, L. The ice period; a period of the history of our globe. *Selections from the Periodical Literature of all Foreign Countries*, 3, 307–326, 1842.
- Agassiz, L. Traces of glaciers under the tropics. Unpublished paper read before the National Assembly of Sciences, Washington, D.C., August 12th, 1866.
- Berner, Robert A. GEOCARB II: A revised model of atmospheric CO_2 over Phanerozoic time. *Am. J. Science*, 294, 56–91, 1994.
- Bodyko, M. I., A. B. Ronov, A. L. Yenshin. *History of the Earth's Atmosphere*, Springer-Berlin, 1987.
- Boville, B. A. and P. R. Gent. The NCAR climate system model, version 1. *J. Clim.*, 11, 1115–1130, 1998.
- Branner, J. C. The supposed glaciation of Brazil, *Journal of Geology*, 1, 753–772, 1893.
- Broecker, Wallace S., A boundary condition on the evolution of atmospheric oxygen, *J. Geophys. Res.*, 75, 3553–3557, 1970.
- Chumakov, N. M., Upper Proterozoic glaciogenic rocks and their stratigraphic significance, *Palaeogeog. Palaeoclim. Palaeoec.*, 51, 319–346, 1981.
- Craig, H., The geochemistry of the stable carbon isotopes, *Geochim. Cosmochim. Acta*, 3, 53, 1953.
- Crowley, T. J., W. T. Hyde and W. R. Peltier, CO_2 levels required for deglaciation of a “Near-Snowball” Earth, *Geophys. Res. Lett.*, 28, 283–286, 2001.
- Dalziel, I. W. D., Overview: Neoproterozoic-Paleozoic geography and tectonics: Review, hypothesis, environmental speculation, *Geol. Soc. Am. Bull.*, 109, 16–42, 1997.
- Deblonde, G. and W. R. Peltier, Simulations of continental ice sheet growth over the last glacial-interglacial cycle: Experiments with a one level seasonal energy balance model including realistic geography, *J. Geophys. Res.*, 96, 9189–9215, 1991.
- Deblonde, G., W. T. Hyde and W. R. Peltier, Simulations of continental ice sheet growth over the last glacial-interglacial cycle: experiments with a one level seasonal energy balance model including seasonal ice-albedo feedback, *Global Planet. Change*, 98, 37–55, 1992.
- Deblonde, G. and W. R. Peltier, Late Pleistocene ice-age scenarios based upon observational evidence, *J. Climate*, 6, 709–727, 1993.
- Eyles, N. and N. Januszczak, “Zipper-Rift”: a tectonic model for Neoproterozoic glaciations during the breakup of Rodinia after 750 Ma, *Earth Sc. Rev.*, in press, 2003.
- Flato, G. M. and W. D. Hibler, Modelling pack ice as a cavitating fluid, *J. Phys. Oceanogr.*, 22, 626–651, 1992.
- Gent, P. R. and J. C. McWilliams, Isopycnal mixing in the ocean circulation model, *J. Phy. Oceanogr.*, 20, 150–155, 1990.
- Gent, P. R., J. Willebrand, J. McDougall and J. C. McWilliams, Parameterizing eddy-induced tracer transports in an ocean circulation model, *J. Phy. Oceanogr.* 25, 463–474, 1995.
- Gent, P. R., F. O. Bryan, G. Danabasoglu, S. C. Doney, W. R. Holland, W. G. Large and J. C. McWilliams, The NCAR climate system model global ocean component, *J. Clim.*, 11, 1287–1306.
- Harland, W. B. and K. N. Herod, Glaciations through time. In Wright, A. E. and Moseley, F. (eds.), *Ice Ages: Ancient and Modern*. Pp. 189–216. Seel House Press, Liverpool.
- Hoffman, P. F. and D. P. Schrag, The snowball Earth, <http://eps.harvard.edu/people/faculty/hoffman/snowball-paper.html>, 1999.
- Hoffman, P. F. and D. F. Schrag, Snowball Earth. *Scientific American*, 282, 68–75, 2000.
- Hoffman, P. F. and D. P. Schrag, The snowball Earth hypothesis: testing the limits of global change, *Terra Nova*, 14, 129–155, 2002.
- Huybrechts, P. and S. T'Siobbel, Thermomechanical modelling of Northern Hemisphere ice sheets with a two-level mass balance parameterization, *Ann. Glaciol.*, 21, 111–116, 1995.

- Hyde, W. T., T. J. Crowley, S. K. Baum and W. R. Peltier, The Pangean ice-age: Studies with a coupled climate-ice sheet model. *Clim. Dyn.*, 15, 619–629, 1999.
- Hyde, W. T., T. J. Crowley, S. K. Baum and W. R. Peltier, Neoproterozoic “Snowball Earth” simulations with a coupled climate/ice sheet model, *Nature*, 405, 425–430, 2000.
- Hyde, W. T., T. J. Crowley, S. K. Baum and W. R. Peltier, Life, geology and snowball Earth, Reply to comment, *Nature*, 409, 206, 2001.
- IPCC-WG1. Climate change 1995: the science of climate change. In: Houghton et al. (eds). *Contribution of WG1 to the second assessment report of the intergovernmental panel on climate change*. Cambridge University Press, New York, pp. 572.
- Kauffman, A. J., An ice age in the tropics, *Nature*, 386, 227–228, 1997.
- Kiehl, J. T., J. J. Hack, G. B. Bonan, B. A. Boville, D. L. Williamson, P. J. Rasch, The National Center for Atmospheric Research Community Climate Model: CCM3, *J. Clim.*, 11, 1131–1149, 1998.
- Keith, M. L., and J. N. Webber, Carbon and oxygen isotopic compositions of mollusk shells from marine and freshwater environments, *Geochim. Cosmochim. Acta* 28, 1787. 1964.
- Kirschvink, J. L., Late Proterozoic low-latitude global glaciation: the snowball Earth. In J.W. Schopf and C. Klein (eds.), *The Proterozoic Biosphere, A Multi-disciplinary Study*, pp. 51–52, Cambridge University Press.
- Large, W. G., J. C. McWilliams and S. C. Doney, Oceanic vertical mixing: a review and a model with a nonlocal boundary layer parameterization, *Rev. Geophys.*, 32, 363–463.
- North, G. R., J. G. Mengel and D. A. Short, Simple energy balance climate model resolving the seasons and continents: Application to the astronomical theory of the ice ages, *J. Geophys. Res.*, 88, 6576–6586, 1983.
- Payne, A. J. et al., Results from the EISMINT model intercomparison: the effects of thermomechanical coupling. *J. Glaciol.*, 46, 227–238, 2000.
- Peltier, W. R., Earth system history, In M.C. MacCracken and J. S. Perry (eds.), *The Encyclopedia of Global Environmental Change: vol. 1*, pp. 31–60, 2002.
- Peltier, W. R. and L. P. Solheim, The climate of the Earth at Last Glacial Maximum: statistical equilibrium state and a mode of internal variability, *Quat. Sci. Rev.*, 23, 335–357, 2004.
- Rothman, D. H., Atmospheric CO₂ levels for the last 500 million years, *PNAS*, 99, 4167–4171, 2002.
- Rothman, D. H., J. M. Hayes and R. E. Summons, Dynamics of the Neoproterozoic carbon cycle, *PNAS*, 100, 8124–8129, 2003.
- Runnegar, B., Loophole for Snowball Earth, *Nature*, 405, 403–404, 2000.
- Semtner, A. J., A model for the thermodynamic growth of sea-ice in numerical investigations of climate, *J. Phys. Oceanogr.*, 6, 376–389, 1976.
- Tarasov, L. and W. R. Peltier, Impact of thermomechanical ice sheet coupling on a model of the 100 kyr ice age cycle, *J. Geophys. Res.*, 104, 9517–9545, 1999.
- Weatherly, J. W., B. P. Briegleb, W. E. Large, J. A. Muslanik, Sea ice and polar climate in the NCAR-CSM, *J. Clim.*, 11, 1472–1486, 1998.

W. R. Peltier, Department of Physics, University of Toronto, 60 St. George Street, Toronto, Ontario, M5S 1A7 Canada.